Dielectric confinement on exciton binding energy and nonlinear optical properties in a strained $Zn_{1-x_{in}}Mg_{x_{in}}Se/Zn_{1-x_{out}}Mg_{x_{out}}Se$ quantum well

J. Abraham Hudson Mark[1] and A. John Peter[2, †]

[1]Department of Physics, NPR Arts & Science College, Natham, Dindigul-624 401, India
[2]Department of Physics, Government Arts College, Melur-625 106, Madurai, India

Abstract: The band offsets for a $Zn_{1-x_{in}}Mg_{x_{in}}Se/Zn_{1-x_{out}}Mg_{x_{out}}Se$ quantum well heterostructure are determined using the model solid theory. The heavy hole exciton binding energies are investigated with various Mg alloy contents. The effect of mismatch between the dielectric constants between the well and the barrier is taken into account. The dependence of the excitonic transition energies on the geometrical confinement and the Mg alloy is discussed. Non-linear optical properties are determined using the compact density matrix approach. The linear, third order non-linear optical absorption coefficient values and the refractive index changes of the exciton are calculated for different concentrations of magnesium. The results show that the occurred blue shifts of the resonant peak due to the Mg incorporation give the information about the variation of two energy levels in the quantum well width.

Key words: interband emission energy; exciton binding energy; quantum well
DOI: 10.1088/1674-4926/33/9/092001 **EEACC:** 2520

1. Introduction

II–VI based semiconductor heterostructures exhibit an excellent radiative recombination showing a high oscillator strength and density states in lasing process that can be used for light emitting devices, blue laser diodes[1, 2], UV photodetectors[3] and other optoelectronic devices which require a large exciton binding energy. Among II–VI group materials, ZnSe shows the strongest Columbic interaction. Mg based blue green laser diodes were fabricated and demonstrated first[4]. In order to produce blue green light emitters some alkali earth atoms are considered to replace the part of II-B cations in those semiconductors[5]. The band gap and the lattice parameter of $Zn_{1-x}Mg_xSe$ with various Mg concentrations has been investigated previously[6]. Investigation of the pressure dependence of subband transitions in $ZnSe/Zn_{1-x}Mg_xSe$ quantum wells was dealt with by Griebl *et al.*[7], who brought out the different pressure dependence of the elastic constants. A cross-over of heavy hole (hh) and light hole (lh) transition energies has been observed. Further, these alloy systems can be tuned to a suitable wavelength by varying the Mg composition. Hence, these II–VI semiconductor nano-structures are imperative for the potential application of opto-electronic devices.

Very recently exciton states in a shallow ZnSe/ZnMgSe quantum well with 3.6% of Mg content have been investigated experimentally[8]. Excitons and charged excitons have been observed in ZnSe based quantum wells with Mg based barriers[9]. It is well known that the effect of strain plays an important role for any semiconductor heterostructure in which there occurs a lattice mismatch between the inner and outer material and thus, in order to improve its opto-electronic properties, the strain effect must be taken into account[10]. Band offsets of $ZnSe/Zn_{1-x}Mg_xSe$ heterostructures have been investigated by the measurements of optical and photoelectron spectra, with varying Mg content (0.1 to 0.4)[11]. Structural and electronic properties of Mg based wide band gap ternary alloys have been investigated[12, 13]. Various quantities, including lattice parameters, bulk modulus, bandgap, optical bowing, bond iconicity character and effective masses have been obtained for the alloys.

In the present work, we calculate the exciton binding energies due to heavy holes in a $Zn_{1-x_{in}}Mg_{x_{in}}Se/Zn_{1-x_{out}}Mg_{x_{out}}Se$ quantum well, with varying Mg composition, taking into account the dielectric confinement. The interband emission energy as a function of well width and Mg content is investigated. Some non-linear optical properties as a function of photon energy are observed. In Section 2, we briefly describe the method and model used in our calculations of obtained eigen functions and eigen energies of electron states, oscillator strengths and the linear and non-linear optical absorption coefficients. The results and discussion are presented in Section 3. A brief summary and results are presented in the last Section.

2. Model and calculations

2.1. Band offset calculations

An exciton is confined in a $Zn_{1-x_{in}}Mg_{x_{in}}Se$ quantum well sandwiched between two potential barriers of $Zn_{1-x_{out}}Mg_{x_{out}}Se$. The confining potential is considered to be zero and V_0 outside, V_0 depends on the Mg content in the quantum well, whereas we have kept $x_{out} = 0.9$ in the barrier. We estimate the exciton binding energies, the interband emission energies and some non-linear optical properties for various V_h and V_c by varying the Mg composition. The valence and conduction band offset is done by the model solid approach[14]. The heavy hole and light hole band offsets are calculated as the difference between the energies at the top of heavy hole and light hole bands in $Zn_{1-x_{out}}Mg_{x_{out}}Se$ and $Zn_{1-x_{in}}Mg_{x_{in}}Se$. Similarly, the conduction band offset is cal-

† Corresponding author. Email: a.john.peter@gmail.com
Received 26 February 2012, revised manuscript received 16 May 2012

Table 1. Material parameters* used in the calculations.

Parameter	ZnSe	MgSe
m_e^*	0.114	0.202
γ_1	3.94	2.84
γ_2	1	0.43
ε	9.4	8.2
a (nm)	0.567	0.591
C_{11} (GPa)	8.57	7.58
C_{12} (GPa)	5.07	4.86
a (eV)	1.65 −1.0	
b (eV)	−1.8	−1.27
E_g^Γ (eV)	2.719	4

*Ref. [29]

culated as the difference between the energies at the bottom of the conduction bands in $Zn_{1-x_{out}}Mg_{x_{out}}Se$ and $Zn_{1-x_{in}}Mg_{x_{in}}Se$. Thus, the valence band offset related to heavy holes in the $Zn_{1-x_{out}}Mg_{x_{out}}Se/Zn_{1-x_{in}}Mg_{x_{in}}Se/Zn_{1-x_{out}}Mg_{x_{out}}Se$ heterostructure interface is given by

$$\Delta E_{v,hh} = \Delta E^B_{v,hh}(Zn_{1-x_{out}}Mg_{x_{out}}Se) - \Delta E^D_{v,hh}(Zn_{1-x_{in}}Mg_{x_{in}}Se) + \delta E_{v,hh}, \quad (1)$$

where $\Delta E^B_{v,hh}(Zn_{1-x_{out}}Mg_{x_{out}}Se)$ is the unstrained outer barrier material in the barrier, for which we have taken x_{out} as 0.9 and for the well, we have linearly interpolated the other data taken from Table 1. $\Delta E^B_{v,hh}(Zn_{1-x_{in}}Mg_{x_{in}}Se)$ is the strained inner material in the well, and $\delta E_{v,hh}$ is the shift in the heavy hole valence band energy due to strain, which is expressed as

$$\delta E_{v,hh} = a_v(2\varepsilon + \varepsilon_{zz}) - b(\varepsilon_{zz} - \varepsilon), \quad (2)$$

where a_v is the hydrostatic deformation potential in the valence band, b is the shear deformation potential and strain tensors[15] are given by

$$\varepsilon = \frac{a_D - a_B}{a_B}, \quad (3)$$

and

$$\varepsilon_{zz} = -2\frac{C_{12}}{C_{11}}\varepsilon, \quad (4)$$

where a_D and a_B are the lattice constants of the $Zn_{1-x_{out}}Mg_{x_{out}}Se$ barrier and $Zn_{1-x_{in}}Mg_{x_{in}}Se$ well respectively. C_{11} and C_{12} are the elastic constants of the epitaxial layer material. Similarly, the valence band offset for heavy holes is expressed as

$$\delta E_{v,hh} = a_v(2\varepsilon + \varepsilon_{zz}) - \frac{1}{2}\Delta_0 + \frac{1}{4}b(\varepsilon_{zz} - \varepsilon) + \frac{1}{2}\sqrt{\Delta_0^2 + \Delta_0 b(\varepsilon_{zz} - \varepsilon) + \frac{9}{4}[b(\varepsilon_{zz} - \varepsilon)]^2}, \quad (5)$$

where Δ_0 is the sin orbit splitting. The conduction band offset is given by

$$\Delta E_c = \Delta E^B_c(Zn_{1-x_{out}}Mg_{x_{out}}Se) - \Delta E^D_c(Zn_{1-x_{in}}Mg_{x_{in}}Se) + \Delta E_g + \delta E_c, \quad (6)$$

where ΔE_g is band gap energy is given by[16]

$$\Delta E_g = 1.15 + 0.87x + 0.47x^2, \quad (7)$$

and

$$\delta E_c = a_c(2\varepsilon + \varepsilon_{zz}). \quad (8)$$

The V_c and V_h are calculated using the following expression.

$$V_c = E_c^{Zn_{1-x_{out}}Mg_{x_{out}}Se} - E_c^{Zn_{1-x_{in}}Mg_{x_{in}}Se}, \quad (9)$$

$$V_h = E_{hh}^{Zn_{1-x_{out}}Mg_{x_{out}}Se} - E_v^{Zn_{1-x_{in}}Mg_{x_{in}}Se}, \quad (10)$$

where $E_c^{Zn_{1-x_{out}}Mg_{x_{out}}Se}$ and $E_{hh}^{Zn_{1-x_{out}}Mg_{x_{out}}Se}$ are the energies of the conduction and heavy hole bands in the barrier, $E_c^{Zn_{1-x_{in}}Mg_{x_{in}}Se}$ and $E_v^{Zn_{1-x_{in}}Mg_{x_{in}}Se}$ are the energies of the conduction and heavy hole bands in the well.

2.2. Exciton binding energy

The exciton Hamiltonian with the effect of electron–LO phonon interaction in a $Zn_{1-x_{out}}Mg_{x_{out}}Se/Zn_{1-x_{in}}Mg_{x_{in}}Se/Zn_{1-x_{out}}Mg_{x_{out}}Se$ strained quantum well, within the single band effective mass approximation, is given by

$$\hat{H} = -\frac{\hbar^2}{2\mu_+(x)}\frac{1}{\rho}\frac{\partial}{\partial\rho}\rho\frac{\partial}{\partial\rho} - \frac{\hbar^2}{2m_e^*(x)}\frac{\partial^2}{\partial z_e^2} - \frac{\hbar^2}{2m_+(x)}\frac{\partial^2}{\partial z_h^2} - \frac{e^2}{\varepsilon(r)r} + V_e(z_e) + V_h(z_h) + V_{PB}(r) + V_{KT}(r) + E_{self}, \quad (11)$$

where e is the absolute value of the electronic charge, $m^*_{e,h}(x)$ is the Mg-dependent effective mass of electron and hole of $Zn_{1-x}Mg_xSe$, z_e and z_h are the electron and hole co-ordinates along the growth direction of the structure, $V_{e,h}(x)$ is the Mg-dependent strain induced confined potential for electrons and holes, $V_{PB}(r)$ is the effective potential between an electron and a hole, $V_{KT}(r)$ is the effective potential due to the effect of dielectric confinement in the image charge method[17], $\varepsilon(r)$ is the size dependent dielectric function and $r = \sqrt{\rho^2 + (z_e - z_h)^2}$. The μ_+ is the reduced mass of the exciton given by Ref. [18], m_0 is the free electron mass and m_e^* is the electron effective mass. The parameter m_+ is the hole effective mass given by

$$\frac{1}{m_+} = \frac{1}{m_0}(\gamma_1 - 2\gamma_2). \quad (12)$$

The size dependent dielectric function is given by[19, 20]

$$\frac{1}{\varepsilon(r_0)} = \frac{1}{\varepsilon_\infty} - \left[\frac{1}{\varepsilon_\infty} - \frac{1}{\varepsilon_0}\right] \times \left[1 - \frac{\exp(-r_0/\rho_e) + \exp(-r_0/\rho_h)}{2}\right], \quad (13)$$

where r_0 is the mean electron–hole distance, ε_0 and ε_∞ are the static and optical dielectric constants and $\rho_{e,h}$ are given by[21]

$$\rho_{e,h} = \frac{\hbar}{2m^*_{e,h}\omega_{LO}}, \quad (14)$$

where $\hbar\omega_{\mathrm{LO}}$ is the LO phonon energy.

The effect of the exciton and LO phonon interaction is derived by the effective potential (V_{PB}) between the electron and hole along with the self energy term (E_{self}) as given below. The quantum well confinement effective potential of the electron and hole is given by[22]

$$V_{\mathrm{PB}}(r) = -\frac{e^2}{\varepsilon^* r}\left[\frac{C^4}{B^4} - \frac{m_{\mathrm{e}}^* h_{\mathrm{e}}}{\Delta m}\exp\left(-\frac{rA_{\mathrm{e}}}{R_{\mathrm{e}}}\right) + \frac{m_{\mathrm{h}}^* h_{\mathrm{h}}}{\Delta m}\exp\left(-\frac{rA_{\mathrm{h}}}{R_{\mathrm{h}}}\right)\right] - \left(h_\mu + \frac{C^3 r}{2B^3 a_{\mathrm{ex}}}\right)\exp\left(-\frac{rB}{R_\mu}\right), \quad (15)$$

where $\varepsilon^* = (1/\varepsilon_\infty - 1/\varepsilon_{\mathrm{s}})^{-1}$, ε_∞ and ε_s are the optical and static dielectric constants of the well material and Δm is the difference in effective mass of electron and hole. When a well is sandwiched between the barrier materials, the field effect caused by the charge distribution will enhance the Coulomb interaction.

The self energy term is given by[23]

$$E_{\mathrm{self}} = -(\alpha_{\mathrm{e}} g_{\mathrm{e}} + \alpha_{\mathrm{h}} g_{\mathrm{h}} - \alpha_\mu g_\mu)\hbar\omega_{\mathrm{LO}}, \quad (16)$$

where $\hbar\omega_{\mathrm{LO}}$ is the LO phonon energy. The calculation of other material parameters in Eq. (13) and Eq. (14) is followed from Ref. [13].

The effective potential due to the effect of dielectric confinement on the interaction between the electron and the hole is calculated below. The effect of electron–hole confinement in the image charge method is given by the effective potential as[17]

$$V_{\mathrm{KT}}(r) = -\sum_{n=-\infty}^{\infty}\frac{\xi^{|n|}}{\varepsilon_{\mathrm{s}}\sqrt{\rho^2 + (z_{\mathrm{z}} - (-1)^n z_{\mathrm{h}} + nL_{\mathrm{W}})^2}}, \quad (17)$$

where $\xi = (\varepsilon_{\mathrm{s}}^{\mathrm{w}} - \varepsilon_{\mathrm{s}}^{\mathrm{b}})/(\varepsilon_{\mathrm{s}}^{\mathrm{w}} + \varepsilon_{\mathrm{s}}^{\mathrm{b}})$ and $\varepsilon_{\mathrm{s}}^{\mathrm{w}}$ and $\varepsilon_{\mathrm{s}}^{\mathrm{b}}$ are the static dielectric constants of the well and the barrier respectively.

The electron and heavy hole subband energies are computed by numerically solving the equation for a finite quantum well potential. We have chosen the trial wave function for the exciton ground state, within the variational scheme. We take the problem of an exciton in a $Zn_{1-x_{\mathrm{out}}}Mg_{x_{\mathrm{out}}}Se/Zn_{1-x_{\mathrm{in}}}Mg_{x_{\mathrm{in}}}Se/Zn_{1-x_{\mathrm{out}}}Mg_{x_{\mathrm{out}}}Se$ quantum well within the single band effective mass approximation. It is necessary to use a variational approach to calculate the eigen function and eigen value of the Hamiltonian and to calculate the ground state exciton energy using a trial wave function with two variational parameters. Considering the correlation of the electron-hole relative motion, the trial wave function can be chosen as,

$$\Psi(\bar{r}_{\mathrm{e}}, \bar{r}_{\mathrm{h}}) = N f_{\mathrm{e}}(\rho_{\mathrm{e}}, z_{\mathrm{e}})\, f_{\mathrm{h}}(\rho_{\mathrm{h}}, z_{\mathrm{h}})\mathrm{e}^{-\alpha\rho^2}\mathrm{e}^{-\beta z^2}, \quad (18)$$

where N is the normalization constant, f_{e} and f_{h} are ground state solution of the Schrödinger equation for the electrons and holes in the absence of the Coulomb interaction. The above equation describes the correlation of the electron-hole relative motion. α and β are variational parameters responsible for the in-plane correlation and the correlation of the relative motion in the z-direction respectively. By matching the wave functions and the effective mass and their derivatives at boundaries of the quantum well along with the normalization, we fix all the constants except the variational parameters. So the wave function given in Eq. (18) completely describes the correlation of the electron–hole relative motion.

The Schrödinger equation is solved variably by finding $\langle H\rangle_{\min}$, and the binding energy of the exciton in the quantum well is given by the difference between the energy with and without the Coulomb term. First, we concentrate on the calculation of the electronic structure of the ZnMgSe quantum well system by calculating its subband energy (E) and subsequently the exciton binding energy. To calculate the ground-state energies of the heavy excitons, we minimize the expectation values of the Hamiltonian (Eq. (11)) calculated using a trial function with two variational parameters (Eq. (18)).

The binding energy of the excitonic system is defined as

$$E_{\mathrm{exc}}(x) = E_{\mathrm{e}} + E_{\mathrm{h}} - \langle H_{\mathrm{exc}}(\rho, z)\rangle_{\min}, \quad (19)$$

where $E_{\mathrm{e,h}}$ is the sum of the free electron and the free hole self-energies in the same quantum well.

The Hamiltonian of an exciton consisting of a single electron part (H_{e}), the single hole part (H_{h}) and the Coulomb interaction term between electron–hole pair is given by

$$H_{\mathrm{exc}}(x) = H_{\mathrm{e}} + H_{\mathrm{h}} + V_{\mathrm{e,h}} - \frac{e^2}{\varepsilon\,|r|} + E_{\mathrm{self}} + V_{\mathrm{PB}}(r) + V_{\mathrm{KT}}(r), \quad (20)$$

where all the terms are defined as earlier. The Mg-depended band gap of $Zn_{1-x}Mg_xSe$ is explained as previously. It is inferred that the direct band gap of ZnSe increases linearly with Mg concentration. Thus the incorporation of Mg into ZnSe will significantly change its band gap. The ground state energy of the exciton in the $Zn_{1-x}Mg_xSe$ quantum well is calculated by using the following equation

$$E_{\mathrm{exc}} = \min_{\alpha,\beta}\frac{\langle\psi_{\mathrm{exe}}\,|H_{\mathrm{exc}}|\,\psi_{\mathrm{exc}}\rangle}{\langle\psi_{\mathrm{exc}}\,|\psi_{\mathrm{exc}}\rangle}. \quad (21)$$

The ground state exciton binding energy E_{b} and the interband emission energy E_{ph} associated with the exciton is calculated using the following equation

$$E_{\mathrm{b}} = E_{\mathrm{e}} + E_{\mathrm{h}} - E_{\mathrm{exc}}, \quad (22)$$

$$E_{\mathrm{ph}} = E_{\mathrm{e}} + E_{\mathrm{h}} + E_{\mathrm{g}}^{\Gamma}(x) - E_{\mathrm{exc}}, \quad (23)$$

where E_{e} and E_{h} are the confinement energies of the electron and hole respectively. $E_{\mathrm{g}}^{\Gamma}(x)$ is the Mg-dependent band gap energy of $Zn_{1-x}Mg_xSe$ material.

2.3. Absorption coefficients and refraction index changes

For any electronic system transitions, these calculations are imperative to compute the different optical properties. However, the dipole transitions are allowed using the selection rules $\Delta l = \pm 1$ where l is the angular momentum quantum number. In addition to that the oscillator strength which is related to the dipole transition, is expressed as

$$P_{\mathrm{fi}} = \frac{2m^*}{\hbar^2}\Delta E_{\mathrm{fi}}\,|M_{\mathrm{fi}}|^2, \quad (24)$$

where $\Delta E_{\mathrm{fi}} = E_{\mathrm{f}} - E_{\mathrm{i}}$ refers the difference of the energy between the lower and upper states. $M_{\mathrm{fi}} = 2\langle f | \boldsymbol{R} | i \rangle$ is the electric dipole moment of the transition from i state to f state in the quantum well width. Here, we have considered the selection rule, $\Delta l = \pm 1$ which determines the fine state of the electron after absorption. Hence the state, $L = 0$, is taken as the ground state and the state, $L = 1$, is taken as the final state. The observation of oscillator strength is imperative especially in the study of optical properties and they are related to the electronic dipole allowed absorptions. Moreover, the outcome of the results will give an insight into the fine structure of the optical absorption.

The optical absorption calculations are based on the Fermi Golden rule from which the total absorption coefficient is given by[24]

$$\alpha(\omega, I) = \alpha_1(\omega) + \alpha_3(\omega, I) = \omega\sqrt{\frac{\mu_0}{\varepsilon_{\mathrm{r}}}}\,\mathrm{Im}\left[\varepsilon_0\chi_1(\omega) + \varepsilon_0\chi_3(\omega)I\right], \tag{25}$$

where μ_0 is the permeability of the material, ε_{r} is the real part of the permeability and I is the incident light intensity. $\chi_1(\omega)$ and $\chi_3(\omega)$ describe the linear and nonlinear contribution to the polarization with the same frequency of the incident field.

The optical absorption coefficient is given by

$$\alpha_1(\omega) = \frac{4\pi\alpha_{\mathrm{f}}\sigma_{\mathrm{s}}}{n_{\mathrm{r}}e^2}\hbar\omega\,|M_{\mathrm{fi}}|^2\,\delta(E_{\mathrm{f}} - E_{\mathrm{i}} - \hbar\omega), \tag{26}$$

and

$$\alpha_3(\omega, I) = -\frac{32\pi^2\alpha_{\mathrm{f}}\sigma_{\mathrm{s}}I}{n_{\mathrm{r}}^2e^2\hbar\Gamma_{\mathrm{ff}}}\hbar\omega\,|M_{\mathrm{fi}}|^2\,\delta(E_{\mathrm{f}} - E_{\mathrm{i}} - \hbar\omega) \times \left\{1 - \frac{|M_{\mathrm{ff}} - M_{\mathrm{ii}}|^2}{4\,|M_{\mathrm{fi}}|^2} \times \frac{[(\hbar\omega - E_{\mathrm{fi}})^2 - (\hbar\Gamma_{\mathrm{fi}})^2 + 2E_{\mathrm{fi}}(E_{\mathrm{fi}} - \hbar\omega)]}{E_{\mathrm{fi}}^2 + (\hbar\Gamma_{\mathrm{fi}})^2}\right\}, \tag{27}$$

where σ_{s} is the electron density of the quantum well, n_{r} is the refractive index of the semiconductor, ω is the angular frequency of the incident photon energy, α_{f} is the fine structure constant and E_{i} and E_{f} denote the confinement energy levels for the ground and first excited states, respectively. The above two equations are linear and third order nonlinear optical absorption coefficients.

From Eqs. (26) and (27), the energy-conserving delta function by the Lorentzian is given by

$$\delta(E_{\mathrm{f}} - E_{\mathrm{i}} - \hbar\omega) = \lim_{\Gamma\to 0}\frac{\Gamma}{\pi(E_{\mathrm{f}} - E_{\mathrm{i}} - \hbar\omega)^2 + \Gamma^2}, \tag{28}$$

where Γ is the line width of the exciton.

The susceptibilities are related to the refractive index changes as

$$\frac{\Delta n(\omega)}{n_{\mathrm{r}}} = \mathrm{Re}\left[\frac{\chi(\omega)}{2n_{\mathrm{r}}^2}\right], \tag{29}$$

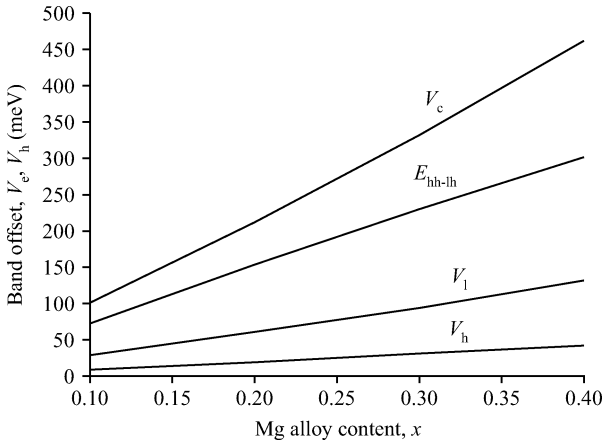

Fig. 1. Variation of conduction (V_{c}), heavy hole (V_{h}), light hole (V_{l}) and energy splitting between heavy and light hole bands ($E_{\mathrm{hh-lh}}$) in a $Zn_{1-x_{\mathrm{out}}}Mg_{x_{\mathrm{out}}}Se/Zn_{1-x_{\mathrm{in}}}Mg_{x_{\mathrm{in}}}Se/Zn_{1-x_{\mathrm{out}}}Mg_{x_{\mathrm{out}}}Se$ quantum well as a function of x for a well width of 100 Å.

where n_{r} is the refractive index of the material. The analytic expression of the linear and nonlinear changes in the refractive index are given by

$$\frac{\Delta n_{(1)}(\omega)}{n_{\mathrm{r}}} = \frac{\sigma_{\mathrm{s}}e^2}{2\varepsilon_{\mathrm{r}}}\,|M_{\mathrm{fi}}|^2\,\frac{\hbar\omega_{\mathrm{fi}} - \hbar\omega}{(E_{\mathrm{fi}} - \hbar\omega)^2 - (\hbar\Gamma_{\mathrm{fi}})^2}, \tag{30}$$

and

$$\frac{\Delta n_{(3)}(\omega)}{n_{\mathrm{r}}} = -\frac{\mu_0 cI}{4\varepsilon_{\mathrm{r}}n_{\mathrm{r}}^2}\frac{\sigma_{\mathrm{s}}e^4\,|M_{\mathrm{fi}}|^4}{[(E_{\mathrm{fi}} - \hbar\omega)^2 + (\hbar\Gamma_{\mathrm{fi}})^2]^2} \times \left\{4\,|M_{\mathrm{fi}}|^2\,(E_{\mathrm{fi}} - \hbar\omega) - \left[\,|M_{\mathrm{ff}} - M_{\mathrm{ii}}|^2 \times \frac{E_{\mathrm{fi}}(E_{\mathrm{fi}} - \hbar\omega_{\mathrm{fi}})^2 - (\hbar\Gamma_{\mathrm{fi}})^2 3(E_{\mathrm{fi}} - 2\hbar\omega)}{E_{\mathrm{fi}}^2 + (\hbar\Gamma_{\mathrm{fi}})^2}\right]\right\}. \tag{31}$$

Hence the total refractive index change is given by

$$\frac{\Delta n(\omega)}{n_{\mathrm{r}}} = \frac{\Delta n_{(1)}(\omega)}{n_{\mathrm{r}}} + \frac{\Delta n_{(3)}(\omega)}{n_{\mathrm{r}}}. \tag{32}$$

3. Results and discussion

All the material parameters values used in the present numerical calculations are linearly interpolated from the date of ZnSe and MgSe given in Table 1. The atomic units have been followed in the determination of electronic charges and the wave functions in which the electronic charge and Planck's constant have been assumed as unity. The effective masses of the heavy and light holes in the z-direction are calculated as $m_+ = 1/(\gamma_1 - 2\gamma_2)$ and $m_+ = 1/(\gamma_1 + 2\gamma_2)$ respectively. All the relevant parameters have been obtained by a linear interpolation of ZnSe and MgSe parameters. $T(Zn_{1-x}Mg_xSe) = (1-x)T\,ZnSe + xT\,MgSe$, where T refers to various physical parameters used in our calculations.

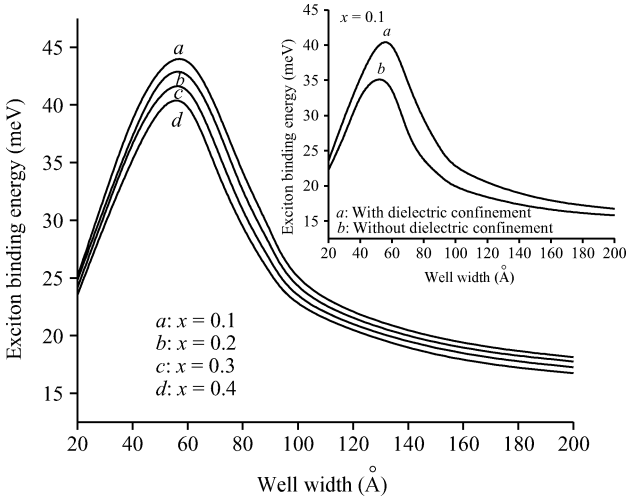

Fig. 2. Variation of exciton binding energy as a function of well width of a $Zn_{1-x_{out}}Mg_{x_{out}}Se/Zn_{1-x_{in}}Mg_{x_{in}}Se/Zn_{1-x_{out}}Mg_{x_{out}}Se$ quantum well for various Mg incorporations with the inclusion of the dielectric confinement. The inserted figure shows the exciton binding energy with and without considering the dielectric confinement for $x = 0.1$.

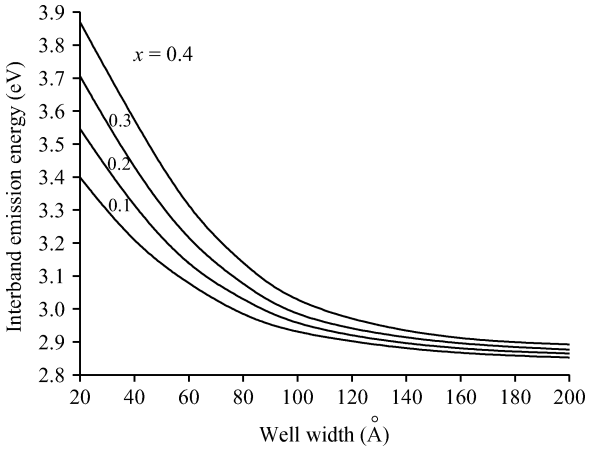

Fig. 3. Variation of interband emission energy as a function of well width for various compositions of Mg in a $Zn_{1-x_{out}}Mg_{x_{out}}Se/Zn_{1-x_{in}}Mg_{x_{in}}Se/Zn_{1-x_{out}}Mg_{x_{out}}Se$ quantum well.

Figure 1 displays the variation of conduction (V_c), heavy hole (V_h), light hole (V_l) and energy splitting between heavy and light hole bands (E_{hh-lh}) in a $Zn_{1-x_{out}}Mg_{x_{out}}Se/Zn_{1-x_{in}}Mg_{x_{in}}Se/Zn_{1-x_{out}}Mg_{x_{out}}Se$ quantum well as a function of x for a constant well width of 100 Å. It is observed that both V_c and V_h increase with Mg concentration. V_{lh} is found to be greater than V_{hh} due to the induced tensile strain. Further, it is observed that the lattice constant of the well material ($Zn_{1-x_{out}}Mg_{x_{out}}Se$) is greater than that of the barrier ($Zn_{1-x_{in}}Mg_{x_{in}}Se$). Hence, the tensile strain will be induced in the well material. Also, the energy splitting between the heavy and light hole bands increases with increasing x due to the increase in induced compressive strain[25].

Figure 2 displays the variation of exciton binding energy as a function of well width of the $Zn_{1-x_{out}}Mg_{x_{out}}Se/Zn_{1-x_{in}}Mg_{x_{in}}Se/Zn_{1-x_{out}}Mg_{x_{out}}Se$ quantum well for various Mg incorporations with the inclusion of the dielectric confinement. The insert figure shows the exciton binding energy with and without consideration of the dielectric confinement for $x = 0.1$. It is observed that the binding energy increases first with decreasing well width and reaches the maximum value for a critical well size before rapidly decreasing when the well width is still reduced for all cases of Mg incorporation in ZnSe material. This is because an increase in the well width results in a spreading of the wave function which causes a lowering in the binding energy and the contribution of confinement is dominant for smaller well width, making the electron unbound, and it ultimately tunnels through the barrier. Eventually, the electron and hole wave functions penetrate into the barrier for narrow wells. Moreover, the variation in Mg composition causes the increase in the barrier height of the quantum well and hence, the exciton binding energy increases with the Mg composition whereas the enhancement of exciton energy with the reduction of well width is due to the spatial confinement. All our calculations include the effect of dielectric confinement and the size dependent dielectric function. The insert figure brings out the effects of PB potential including the dielectric mismatch. It is found that the exciton binding energy obtained using the static screened Coulomb potential is lower than the exciton binding energy with the inclusion of the effective potential. It is observed that the dielectric mismatch effect enhances the exciton binding energy. It implies that the effect of the dielectric mismatch on the exciton binding energy is very important in low dimensional semiconductor heterostructures. Hence, it is concluded that dielectric confinement due to the image charge potential enhances the exciton binding energy[26].

Figure 3 displays the variation of interband emission energy as a function of well width for various compositions of Mg in a $Zn_{1-x_{out}}Mg_{x_{out}}Se/Zn_{1-x_{in}}Mg_{x_{in}}Se/Zn_{1-x_{out}}Mg_{x_{out}}Se$ quantum well. All the calculations have been made with the inclusion of dielectric mismatch. It is noted that the interband emission energy decreases monotonically as the well width is increased for all the Mg content. This is due to the confinement of the electron–hole with respect to the z-plane when the well width is increased. Moreover it is clearly shown that the effect of bound exciton has influence on the interband emission energy. This representation clearly brings out the quantum size effect. The magnitude of the interband emission energy increases with Mg incorporation into the ZnSe material, and is more for all well widths due to the increase in barrier height and exciton binding energy.

Figure 4 shows the variation of the absorption coefficient as a function of photon energy for two different well widths of a $Zn_{1-x_{out}}Mg_{x_{out}}Se/Zn_{1-x_{in}}Mg_{x_{in}}Se/Zn_{1-x_{out}}Mg_{x_{out}}Se$ quantum well for various Mg contents and the insert figure shows the variation of absorption coefficients as a function of photon energy with and without the inclusion of the dielectric confinement effect for a constant Mg alloy content ($x = 0.2$). Here, we observe that the variation of magnitude of an absorption coefficient becomes more when the Mg-incorporation is taken into account. Further, we notice that the increase in linear variation of the resonant absorption coefficient is observed with the Mg incorporation. This is because the exciton binding energy increases with the Mg content eventually increasing the barrier

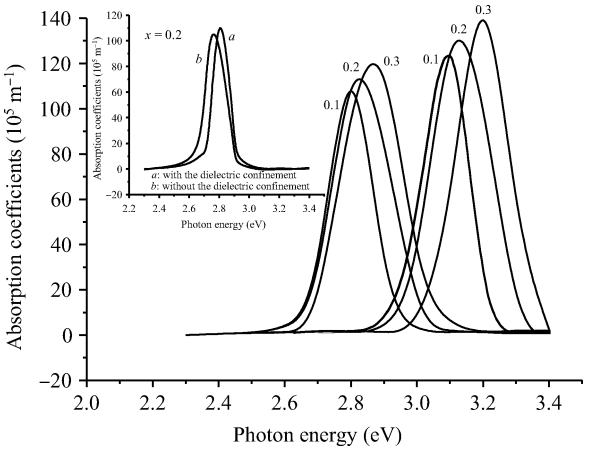

Fig. 4. Variation of the absorption coefficient as a function of photon energy for two different well widths of a $Zn_{1-x_{out}}Mg_{x_{out}}Se/Zn_{1-x_{in}}Mg_{x_{in}}Se/Zn_{1-x_{out}}Mg_{x_{out}}Se$ quantum well for various Mg contents. The inserted figure shows the variation of absorption coefficients as a function of photon energy with and without the inclusion of dielectric confinement for a constant Mg alloy content ($x = 0.2$).

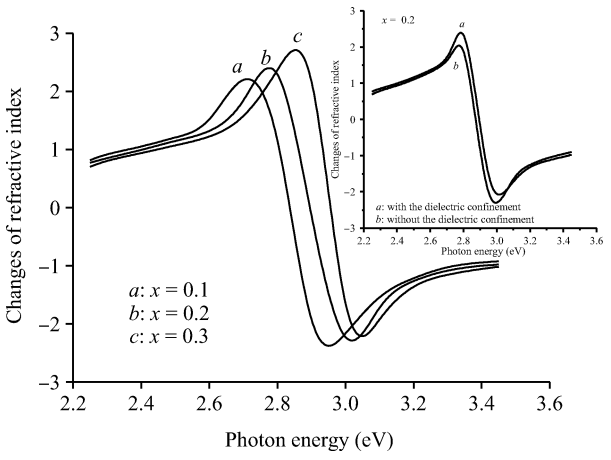

Fig. 5. Variation of total refractive index changes of the exciton confined in a $Zn_{1-x_{out}}Mg_{x_{out}}Se/Zn_{1-x_{in}}Mg_{x_{in}}Se/Zn_{1-x_{out}}Mg_{x_{out}}Se$ quantum well (40 Å) as a function of photon energy, with the influence of Mg concentration. The inserted figure shows the changes of the refractive index as a function of photon energy with and without the dielectric confinement effect.

height. Hence it is concluded that the intensity dependent nonlinear absorption coefficients near the resonant frequencies are important and should be taken into account when studying the optical properties of exciton in the quantum well.

It is observed that the absorption coefficient peak moves to a higher photon energy as the Mg content increases. As the Mg concentration increases, the total absorption coefficient shifts toward higher energies and the magnitude also increases. This implies that the Mg incorporation blue shifts the absorption resonance coefficients in a quantum well, because the spacing between the energy levels increases due to the incorporation of Mg in ZnSe material. The reason for the blue-shift is due to the higher transition energy ($E_2 - E_1$) when the Mg content is increased[27]. Further, we notice that the resonant absorption peak value is found to linearly increase with the Mg content and the energy levels are separated with a reduction of overlap integral due to the increase in dipole matrix. This is because a competition between the energy interval and the dipole matrix element occurs which determines these features. Thus, by increasing the Mg concentration a remarkable blue-shift of the absorption resonant peak is induced, leading to a higher energy interval. Moreover, we notice that the binding energy is higher for when the effect of the dielectric confinement is included for all the well widths due to the enhancement of hydrogen binding energy when the Hamiltonian is included with the polaronic effect. Hence it is concluded that the intensity dependent nonlinear absorption coefficients near the resonant frequencies are important and should be taken into account when studying the optical properties of hydrogenic impurity in the low dimensional heterosystem.

We present the variation of total refractive index changes of the exciton confined in a $Zn_{1-x_{out}}Mg_{x_{out}}Se/Zn_{1-x_{in}}Mg_{x_{in}}Se/Zn_{1-x_{out}}Mg_{x_{out}}Se$ quantum well (40 Å) as a function of photon energy and the influence of Mg concentration, with the constant value of the incident optical intensity (2×10^8 W/m^2) in Fig. 5. The insert figure shows the changes of the refractive index as a function of photon energy with and without the dielectric confinement effect. This figure has been drawn with the combining effects of two components of refractive indices, namely, $\frac{\Delta n_{(1)}(\omega)}{n_r}$ and $\frac{\Delta n_{(3)}(\omega)}{n_r}$ as a function of incident energy for different values of Mg concentration with the constant incident optical intensity. It is observed that as the Mg incorporation increases, the total refractive index changes shift towards the higher values and the magnitude of total refractive index increases. This is because the increase in exciton binding energy occurs with the Mg-composition. It is noticed that a change in the refractive index moves with the higher energy when the effect of the dielectric confinement is included, this is because the enhancement of the binding energy occurs due to the inclusion of the dielectric confinement. Also, it is noticed from the equations of the change of the refractive index that the linear relative change in the refractive index does not depend on photon intensity but on the third order relative change in the refractive index, which changes with photon intensity, and it varies quadratically with the matrix element of the electric dipole moment of the transition. Thus, the nonlinear term must be considered when calculating the refractive index changes of quantum well systems in which the incident light propagates along the z-axis[28]. Thus, the nonlinear term must be considered when calculating the refractive index changes in low dimensional semiconductor systems.

In conclusion, the heavy hole exciton binding energy, interband emission energy and some non-linear optical properties in a $Zn_{1-x_{out}}Mg_{x_{out}}Se/Zn_{1-x_{in}}Mg_{x_{in}}Se/Zn_{1-x_{out}}Mg_{x_{out}}Se$ quantum well have been investigated for various Mg composition. The band offsets have been computed using the Model solid theory. The results bring out the effect of polaron-induced enhancement of the exciton binding energy, which implies that polaronic coupling cannot be neglected while calculating the excitonic properties of these materials. Also, we have calculated the effect of the exciton interacting with confined LO phonons, on its binding energy of a polar semiconduc-

tor in a quantum well with finite potential barriers. The computed 1s heavy hole exciton binding energies are significantly larger, by 6 meV, when the interaction potential V_{AB} is included in the Hamiltonian. Thus, the excitonic Hamiltonian with the inclusion of an effective interaction potential taking into account the polaronic effects have been presented in this paper. In any polar semiconductor, in general, the electron and heavy hole effective masses will be replaced by the corresponding polarnoic masses and the screened Coulomb potential will be replaced by the effective potential in the exciton Hamiltonian. It is found that the band offsets in the $Zn_{1-x_{out}}Mg_{x_{out}}Se/Zn_{1-x_{in}}Mg_{x_{in}}Se/Zn_{1-x_{out}}Mg_{x_{out}}Se$ quantum well heterostructure greatly depends on the Mg alloy content. The exciton binding energy due to heavy holes depends on the well width, Mg content, the strain effect and the dielectric confinement. The occurred blue shifts of the resonant peak due to the Mg incorporation give the information about the variation of two energy levels in the quantum well width. This property makes this material very promising for future potential applications such as fabricating the highly desirable blue green region of an electro-magnetic spectrum in opto-electronic devices.

References

[1] Sun G, Shahzad K, Gaines J M, et al. Room-temperature photo pumped blue lasing in ZnSe–$ZnS_{0.06}Se_{0.94}$ double heterostructures. Appl Phys Lett, 1991, 59: 310

[2] Ichino K, Wu Y H, Kawakami Y, et al. Fabrication of ZnCdSSe alloys by MOMBE and their applications for double-hetero and quantum-well structures. J Cryst Growth, 1992, 117: 527

[3] Cohen M L, Chelikowsky J R. Electronic structure and optical properties of semiconductors. Berlin: Springer,1988

[4] Haase M A, Qiu J, DePuydt J M, et al. Blue-green laser diodes. Appl Phys Lett, 1991, 59: 1272

[5] Pelucchi E, Rubini S, Bonanni B, et al. Structural and electronic properties of wide band gap $Zn_{1-x}Mg_xSe$ alloys. J Appl Phys, 2004, 95: 4184

[6] Jobst B, Hommel D, Lunz U, et al. Molecular beam epitaxial growth and characterization of zinc-blende ZnMgSe on InP (001). Appl Phys Lett, 1996, 69: 97

[7] Griebl E, Stier A, Krenzer M, et al. Investigation of the pressure dependence of subband transitions in ZnSe/$Zn_{1-x}Mg_xSe$ quantum wells by PLE. J Cryst Growth, 1998, 184/185: 853

[8] Pawlis A, Berstermann T, Brüggemann C, et al. Exciton states in shallow ZnSe/(Zn,Mg)Se quantum wells: interaction of confined and continuum electron and hole states. Phys Rev B, 2011, 83: 115302

[9] Astakhov G V, Yakovlev D R, Kochereshko V P, et al. Binding energy of charged excitons in ZnSe-based quantum wells. Phys Rev B, 2001, 65: 165335

[10] Kato Y K, Myers R C, Gossard A C, et al. Current-induced spin polarization in strained semiconductors. Phys Rev Lett, 200, 493: 176601

[11] Wörz M, Griebl E, Reisinger T, et al. Gap energies, exciton binding energies and band offsets in ternary ZnMgSe compounds and ZnSe/ZnMgSe heterostructures. Phys Status Solidi B, 1997, 202: 805

[12] Falke U, Cichos A, Firsztb F, et al. Structural investigations of polytypes in $Zn_{1-x}Mg_xSe$ by transmission electron microscopy and cathodoluminescence. J Cryst Growth, 1998, 184: 1015

[13] Benkabou F, Aourag H, Certier M, et al. Composition dependence of the positron annihilation in $Zn_{1-x}Mg_xSe$. Phys B, 2003, 336: 275

[14] Shahzad K, Olego D, Van de Walle C G. Optical characterization and band offsets in ZnSe–ZnS_xSe_{1-x} strained-layer superlattices. Phys Rev B, 1988, 38: 1417

[15] Wu Y, Ichino K, Kawakawi Y, et al. Estimation of critical thicknesses and band lineups in ZnCdSe/ZnSSe strained-layer system for design of carrier confinement quantum well structure. Jpn J Appl Phys, 1992, 31: 1737

[16] Charifi Z, Hassan F E H, Baaziz H, et al. Structural and electronic properties of the wide-gap $Zn_{1-x}Mg_xS$, $Zn_{1-x}Mg_xSe$ and $Zn_{1-x}Mg_xTe$ ternary alloys. J Phys Condes Matter, 2005, 17: 7077

[17] Kumagai M, Takagahara T. Excitonic and nonlinear-optical properties of dielectric quantum-well structures. Phys Rev B, 1989, 40: 12359

[18] Senger R T, Bajaj K K. Binding energies of excitons in polar quantum well heterostructures. Phys Rev B, 2003, 68: 205314

[19] Nanda K K, Kruis F E, Fissan H, et al. Effective mass approximation for two extreme semiconductors: band gap of PbS and CuBr nanoparticles. J Appl Phys, 2004, 95: 5035

[20] Baskoutas S, Terzis A F, Schommers W. Size-dependent exciton energy of narrow band gap colloidal quantum dots in the finite depth square-well effective mass approximation. J Comput Theor Nanosci, 2006, 3: 269

[21] Pellegrini G, Mattei G, Mazzoldi P. Finite depth square well model: applicability and limitations. J Appl Phys, 2005, 97: 073706

[22] Pollmann J, Büttner H. Effective Hamiltonians and bindings energies of Wannier excitons in polar semiconductors. Phys Rev B, 1977, 16: 4480

[23] Firszt F, Legowski S, Meczynska H, et al. Growth and characterisation of $Cd_{1-x}Mg_xSe$ mixed crystals. J Cryst Growth, 1998, 184: 1053

[24] De Sousa S, Leburton J P, Freire V N, et al. Intraband absorption and Stark effect in silicon nanocrystals. Phys Rev B, 2005, 72: 155438

[25] Onodera C, Shoji T, Hiratate Y, et al. Effect in changes of conduction and valence band offsets on exciton binding energy in $Cd_xZn_{1-x}Se/ZnS_ySe_{1-y}$ single quantum wells. Jpn J Appl Phys, 2007, 46: 248

[26] Onodera C, Yoshida M. Effect of dielectric mismatch on exciton binding energy in ZnS/$Mg_xZn_{1-x}S$ quantum wells. e-J Surf Sci Nanotech, 2010, 8: 145

[27] Firszt F. Luminescence properties of $Mg_xZn_{1-x}Se$ crystals. Semicond Sci Technol, 1993, 8: 712

[28] Xie W. A study of two confined electrons using the Woods-Saxon potential. J Phys: Condens Matter, 2009, 21: 115802

[29] Adachi S. Properties of semiconductor alloys: group-IV, III–V and II–VI semiconductors. John Wiley & Sons Ltd, 2009